



## Particle number size distribution and new particle formation in Xiamen, the coastal city of Southeast China in wintertime



Jing Wang<sup>a,b,c</sup>, Mengren Li<sup>a,b,d,\*</sup>, Lingjun Li<sup>a,b,d</sup>, Ronghua Zheng<sup>a,b</sup>, Xiaolong Fan<sup>a,b,d</sup>, Youwei Hong<sup>a,b,d</sup>, Lingling Xu<sup>a,b,d</sup>, Jinsheng Chen<sup>a,b,d,\*</sup>, Baoye Hu<sup>a,b,e</sup>

<sup>a</sup> CAS Center for Excellence in Regional Atmospheric Environment, Institute of Urban Environment, Chinese Academy of Sciences, Xiamen 361021, China

<sup>b</sup> Key Lab of Urban Environment and Health, Institute of Urban Environment, Chinese Academy of Sciences, Xiamen 361021, China

<sup>c</sup> College of Resources and Environment, Fujian Agriculture and Forest University, Fuzhou 350002, China

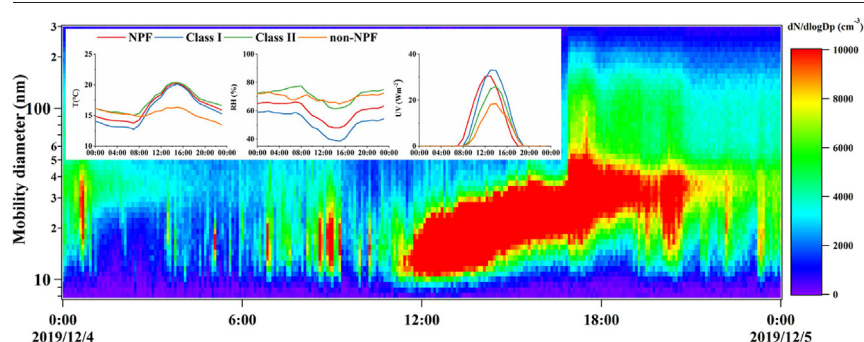
<sup>d</sup> College of Resources and Environment, University of Chinese Academy of Sciences, Beijing 100086, China

<sup>e</sup> Fujian Provincial Key Laboratory of Pollution Monitoring and Control, Minnan Normal University, Zhangzhou 363000, China

### HIGHLIGHTS

- Aitken mode particle contributed about 50% of the particle number concentration.
- High frequency of NPF events was observed in the coastal city Xiamen.
- NPF events mainly showed 'banana' shape in Xiamen wintertime.
- NPF events occurred with high temperature, high radiation, and low relative humidity.

### GRAPHICAL ABSTRACT



### ARTICLE INFO

#### Article history:

Received 24 November 2021

Received in revised form 19 January 2022

Accepted 24 February 2022

Editor: Jianmin Chen

#### Keywords:

Particle size distribution

New particle formation

Formation rate

Growth rate

Meteorological conditions

### ABSTRACT

New particle formation (NPF) has a great impact on regional and global climate, air quality and human health. This study uses a Scanning Mobility Particle Sizer (SMPS) for simultaneous measurement of particle number size distribution (PNSD) in wintertime to investigate NPF in the coastal city of Xiamen. The mean particle number concentration, surface area concentration and volume concentration were  $7.25 \times 10^3 \text{ cm}^{-3}$ ,  $152.54 \mu\text{m}^2 \text{ cm}^{-3}$ , and  $4.03 \mu\text{m}^3 \text{ cm}^{-3}$ , respectively. Particle number concentration was mainly influenced by the nucleation mode and the Aitken mode, whereas the main contributor to particle surface area concentration and volume concentration was accumulation mode particles. The frequency of NPF events occurred was around 41.4% in December 2019. The typical growth rates of new formed particles were  $1.41\text{--}2.54 \text{ nm h}^{-1}$ , and the observed formation rates were  $0.49\text{--}1.43 \text{ cm}^{-3} \text{ s}^{-1}$ . A comparative analysis of conditions between event and non-event days was performed. The results emphasized that air temperature, UV radiation and relative humidity were the most decisive meteorological factors, and NPF events usually occurred under clean atmospheric conditions with low PM concentrations. Although condensation sink was high when NPF event occurred, the level of  $\text{SO}_2$  and  $\text{O}_3$  concentration was also high.

### 1. Introduction

New particle formation (NPF) is a process in which low-volatility vapors emitted from biological or anthropogenic sources condenses to form thermodynamically stable molecular clusters, and then grow into larger particles through condensation with other vapors or particles collisions

\* Corresponding authors at: Institute of Urban Environment, Chinese Academy of Sciences, 1799 Jimei Road, Xiamen 361021, China.

E-mail addresses: [mrlj@iue.ac.cn](mailto:mrlj@iue.ac.cn) (M. Li), [jschen@iue.ac.cn](mailto:jschen@iue.ac.cn) (J. Chen).

(Holmes, 2007). Aerosol particles can directly affect the Earth's radiation balance by interacting with solar radiation, and newly formed particles continue to grow to sizes where they become cloud condensation nuclei (CCN) and then change the physical properties of cloud droplets and indirectly affect climate change, which is one of the major uncertainties in global climate models (Boucher et al., 2013). In addition, aerosol particles produced by new particles formation can enter the body through the skin, lungs and gastrointestinal tract and may have serious side effects on human health (Nel et al., 2006; Oberdorster et al., 2005; Penttinen et al., 2001). To better understand the impact of NPF, especially the role it plays in climate change, a large number of researches have been carried out across different temporal and spatial scales.

Particle number size distribution (PNSD) refer to the variation of particle number concentration (PN) with particle size in a specific aerosol system, which is a key parameter to characterize the source and evolution characteristics of atmospheric particles (Hussein et al., 2004; Wu et al., 2008). In the present study, whether NPF events occur in the atmosphere is judged by the characteristics of PNSD (Wang et al., 2013a). The PNSD of NPF event is characterized by explosive growth of number concentration in nucleation mode, and these particles will continue to grow to a larger size. According to the PNSD observed in actual atmosphere, Hussein et al. (2005a, 2005b) modified the results given by Whitby (1978) to define the modal distribution of particulate matter as four modes: nucleation mode, Aitken mode, accumulation mode and coarse mode. Among them, nucleation mode and Aitken mode are particularly important for studying the nucleation and subsequent growth process of new atmospheric particles. Currently, Differential/Scanning Mobility Particle Sizer (D/SMPS) is the most widely used particle size spectrometer. Its measuring range spans a variety range of size ranges, covering the main stages of new particle formation and growth. And it is of great significance to study whether NPF events occur and their characteristics, such as formation rate (FR) and growth rate (GR).

Since the 1990s, numerous field observations of nucleation and growth of atmospheric particles have been made observed worldwide in different types of locations, including forests (Kammer et al., 2018; Kulmala et al., 2001; Wiedensohler et al., 2019), mountains (Lv et al., 2018; Sellegri et al., 2019), coastal regions and marine (Hoffmann et al., 2001; O'Dowd et al., 2002; Takegawa et al., 2020), rural and suburban (Bae et al., 2010; Hakala et al., 2019; Wang et al., 2019), and urban areas (Qiao et al., 2021; Wehner et al., 2004; Zhu et al., 2021; Zimmerman et al., 2020). The first observations focused on Europe, at the Mace Head coastal site in Ireland (O'Dowd et al., 1998; O'Dowd et al., 2002) and Hyytiälä forest site in Finland (Dal Maso et al., 2005; Kulmala et al., 1998) mainly focused on the NPF events in clean areas, which usually showed a classic “banana-type” growth trend in the PNSD spectrum. Based on these two observations, subsequent field observations were made at the densely populated urban site of San Pietro Capofiume (Hamed et al., 2007), where high formation and growth rates are typical of polluted areas. Research on new particles formation is late in China, field observation was conducted in Beijing and observed NPF events with high frequency for the first time in China (Wu et al., 2007), and then NPF events are divided into “clean” and “polluted”, resulting that the atmosphere NPF events in this region usually occurs in sunny days with lower relative humidity, and the occurrence frequency is highest in spring and lowest in summer.

Current studies suggest that atmospheric nucleation is triggered by intense solar radiation, photo-oxidation of atmospheric gases, and exceptionally high concentrations of low-volatility vapors (Wang et al., 2017). Sulfuric acid is considered to be the most critical gaseous precursor involved in nucleation due to its lower vapor pressure (Sipila et al., 2010). Other low-volatile vapors (e.g. organics) can also drive nucleation, resulting in clusters that are further stabilized in the presence of base compounds (ammonia and amines) or ions (Kirkby et al., 2016). Atmospheric nucleation occurs all the time and everywhere (Kulmala et al., 2017), and the nucleated clusters grow into larger nanoparticles through condensation, coagulation, and other processes, or are removed by collision with pre-existing larger particles. Sulfuric acid, ammonia and organics have made

an important contributions to the growth of newly formed particles in the atmosphere (Kerminen et al., 2018), and the condensation of sulfuric acid contributes significantly to the initial growth process and sometimes dominates, while the contribution of organics becomes increasingly important as particle size increases (Chu et al., 2019; Kulmala et al., 2016), high concentrations of growth factors contribute to the growth of nanoclusters to the detected size. Pre-existing aerosol particles act as a sink of nucleation precursors and nucleation clusters, thus inhibiting the occurrence of NPF events (McMurry and Friedlander, 1979). However, under the condition of atmospheric complex pollution in China, the condensation sink level is high, and NPF events with high FR is still frequently observed.

The particle size distribution, the characteristics of NPF events and their influencing factors under different atmospheric backgrounds have great differences. Relevant domestic researches on atmospheric particle size distribution, and NPF mainly concentrated in the north China plain, the Yangtze River delta and the Pearl River delta area. While the literature is rich with the numerous studies focusing on NPF events and these characteristics in many places around the world, few studies were conducted around southeast coastal cities, especially in the urban atmosphere with light pollution.

Xiamen, located in the intersection between the land and sea area, is a rapid developing city in southeast China. Due to the large number of populations gathering and the rapid economic growth, the environment of coastal urban presents a composite pollution situation such as enhanced atmospheric oxidation and frequent occurrence of haze pollution. Influenced by monsoon, sea-land breeze, sea salt and other factors, the composition and source of atmospheric fine particulate matter are more complex, and its formation and evolution mechanism are still unclear. Particle size distribution is the most important characteristic parameter to describe particulate matter, and the NPF event has been proved to be one of the inducing factors for the frequent occurrence of urban haze weather in winter (Guo et al., 2014; Tang et al., 2021).

This study used a scanning mobility particle sizer (SMPS) to carry out observation concerning on particle size distribution during December 2019 in the coastal city of Xiamen in Southeast China. The main purpose is to characterize particle size distribution, and analyze NPF events and favorable conditions for NPF events in Xiamen wintertime. These results will provide a scientific basis for revealing the formation and growth mechanism of new particles in the southeast coastal area of China, and to provide the references for the control and treatment of particle pollution.

## 2. Methodology

### 2.1. Observation site and instrumentation

The observation site is situated on the rooftop of a building in the Institute of Urban Environment, Chinese Academy of Sciences (IUE, CAS) (118°03'E, 24°36'N, 80 m a.s.l), located in the geometric center of Xiamen, close to Jimei Avenue and Haixiang Avenue with large traffic flow. Hence, the study area would be affected by traffic emissions. The monitoring site is a representative urban site, without significant industrial sources nearby. The observations were conducted consecutively from the 1st to the 31st December 2019.

A Scanning Mobility Particle Sizer (SMPS, model 3938 L50, TSI Inc., USA), coupled with an aerosol neutralizer, a Differential Mobility Analyzer (DMA, model 3082, TSI Inc., USA) and a butanol-based Condensation Particle Counter (CPC, model 3750, TSI Inc., USA), was employed to continuously measure the PN and PNSD in the range of 7–300 nm at a 5-min scan interval during the sampling period. After the impactor removes the large particles larger than the set range of the instrument, the particles are charged by the neutralizer and reach charge balance, then charged aerosols enter DMA and are separated based on their electrical mobility, and finally continue to the external CPC to be counted.

DMA with a bipolar charger is used to produce monodisperse aerosols of known size (Liu and Pui, 1974). Charged particles enter DMA, and particles with different electrical mobility reach different positions in DMA.

Therefore, only particles with a narrow range of electrical mobility can be excluded through the slit at the bottom of DMA to obtain monodisperse aerosols, and then different particle sizes were obtained by varying the voltage of the DMA (TSI manual). And CPC placed downstream of the classifier measures PN per size exiting the DMA by counts single particles. In this CPC, particles pass through saturated vapors of n-butyl alcohol (butanol), and when the liquid condenses on the surface of the particles, they quickly grow to a size that can be detected by optical detector where they are counted easily (TSI manual). In this study, the CPC uses reagent grade of butanol as the working fluid for particle growth.

The flow rate of the sample air and the sheath air were 1.0 and 10.0 L  $\text{min}^{-1}$ , respectively. The relative humidity within the system was kept below 50% by adding a silica-gel dryer in the inlet line and the sheath air cycle. The data were corrected for losses due to diffusion within the inlet line and multiple charge effect.

Hourly  $\text{PM}_{2.5}$  mass concentrations were measured by a Tapered Element Oscillating Microbalance (TEOM1405, Thermo Scientific Corp., USA). Chemical composition of water-soluble inorganic ions ( $\text{SO}_4^{2-}$ ,  $\text{NO}_3^-$ ,  $\text{NH}_4^+$ ,  $\text{Cl}^-$ ,  $\text{Ca}^{2+}$ ,  $\text{K}^+$ ,  $\text{Mg}^{2+}$ ,  $\text{Na}^+$ ) in  $\text{PM}_{2.5}$  were measured by Monitor for AeRosol and GaAses (MARGA ADI 2080; Metrohm Applikon B.V.; Netherlands) with one-hour resolution. Gaseous pollutants (carbon oxide, ozone, sulfur dioxide, and nitrogen dioxide) were determined by online Thermo Instruments TEI 48i, 49i, 43i, and 42i (Thermo Scientific Corp., USA). Ambient meteorological parameters, including air temperature, relative humidity (RH), wind speed and wind direction were continuously monitored using the ultrasonic weather station instrument (150WX, Airmar, USA).

## 2.2. Data analysis

### 2.2.1. NPF event classification

The process of NPF includes nucleation and growth. The particles were nucleated at critical sizes of approximately  $1.5 \pm 0.4$  nm (Kulmala et al., 2012), and then could grow to larger particle size. The detection range of SMPS was between 7 nm and 300 nm in our study. Due to the absence of particle data on Dec. 1st and Dec. 2nd, only 29 days were available for analysis.

In this study, particles were classified into three diameter modes: nucleation mode (<25 nm), Aitken mode (25–100 nm) and accumulation mode (>100 nm) (Hussein et al., 2020; Kalkavouras et al., 2020; Shen et al., 2021). We use  $N_{\text{nuc}}$ ,  $N_{\text{Ait}}$ ,  $N_{\text{accu}}$ , and  $N_{\text{total}}$  to represent the number concentration of nucleation mode particle (7–25 nm), Aitken mode particle (25–100 nm), accumulation mode particle (100–300 nm), and total particles (7–300 nm), respectively. An NPF event is determined from the visual analysis of PNSD data as described by Dal Maso et al. (2005). If a new mode of particle appeared in the nucleation mode is observed to prevail over several hours and the mode shows clear signs of growth, a day can be classified as an NPF event day. Apart from NPF days, all other days are classified as non-events and undefined. Non-event days were determined when there is clearly no indication of NPF or none of the abovementioned criteria are fulfilled. In addition, days that cannot meet the criteria to be identified as either events or non-events are classified as undefined, and they are characterized by some particles appear in the nucleation but no clear signs of growth, or the observation of growth not within the nucleation mode. In the process of NPF event classification, the  $N_{\text{nuc}}$  tends to increase in the morning and evening peak, and the influence of traffic emissions on NPF events will be discussed in Section 3.

### 2.2.2. Calculation of condensation sink, growth rate, formation rate

The GR is defined as the temporal change rate of particle size, and GR can be estimated by the temporal variation of the geometric mean diameter (GMD) in the nucleation mode (7–25 nm) (Hussein et al., 2005a; Kulmala et al., 2012; Wu et al., 2021), calculated as:

$$GR = \frac{GMD}{t} \quad (1)$$

The formation rate (FR) is defined as the flux of changes in particle number concentration within the nucleation mode size range (7–25 nm) (Hussein et al., 2008; Kulmala et al., 2004). FR can be estimated by the temporal change rate of nucleation mode particle number concentration ( $dN_{\text{nuc}}/dt$ ), the loss caused by collision process ( $CoagS_{\text{nuc}} \cdot N_{\text{nuc}}$ ) and growth process ( $GR \cdot N_{\text{nuc}} / \Delta dp$ ), and expressed as (Dal Maso et al., 2005; Kulmala et al., 2012):

$$FR = dN_{\text{nuc}}/dt + CoagS_{\text{nuc}} \cdot N_{\text{nuc}} + GR \cdot N_{\text{nuc}} / dp \quad (2)$$

The condensation sink (CS) reflects the rate of condensable vapors condensing on the surface of preexisting particles in the atmosphere (Wu et al., 2021). CS is calculated as (Dal Maso et al., 2005):

$$CS = 2\pi D \sum \beta_m(D_{p,i}) D_{p,i} N_i \quad (3)$$

where  $D_{p,i}$  is the particle size and  $N_i$  is the PN.  $D$  is the diffusion coefficient of sulfuric acid in this study (Wu et al., 2021).

## 2.3. Quality assurance and quality control

The original PNSD data measured by SMPS need to be corrected to reflect the actual number concentration of atmospheric particles, among which the most critical correction is multi-charge correction and diffusion loss correction (Shang et al., 2018).

Each instrument used in our study was calibrated regularly. In addition to the necessary calibration, each instrument was maintained by a special person who checked the operating status and data quality of the instrument daily to ensure the accuracy of the data. Based on our previous research, maintenance and accuracy of all on-line instruments have been verified.

## 3. Results and discussion

### 3.1. Overview of particle number size distributions

During the observation period, the mean total particle surface area concentration was  $(152.34 \pm 79.97) \mu\text{m}^2 \text{cm}^{-3}$ , mainly composed of accumulation mode particles ( $115.00 \mu\text{m}^2 \text{cm}^{-3}$ , 75.4%) and followed by Aitken mode particles ( $34.95 \mu\text{m}^2 \text{cm}^{-3}$ , 23.0%). The mean total particle volume concentration was  $(4.03 \pm 2.19) \mu\text{m}^3 \text{cm}^{-3}$ , which is predominantly affected by accumulation mode particles ( $3.36 \mu\text{m}^3 \text{cm}^{-3}$ , 98.2%). The statistical analysis of particle number concentration, surface area concentration and volume concentration during the measurement period were summarized in Table 1.

The monthly mean  $N_{\text{total}}$  was  $7.25 \times 10^3 \text{cm}^{-3}$ , varied from  $9.85 \times 10^2$  to  $3.51 \times 10^4 \text{cm}^{-3}$ , which is lower than an urban site of Guangzhou city ( $0.02\text{--}10 \mu\text{m}$ ,  $(2.9 \pm 1.1) \times 10^4 \text{cm}^{-3}$ ) and an urban Middle Eastern environment ( $0.01\text{--}10 \mu\text{m}$ ,  $6.5 \times 10^3\text{--}7.7 \times 10^4 \text{cm}^{-3}$ ) (Hussein et al., 2019; Yue et al., 2010). The mean  $N_{\text{Nuc}}$ ,  $N_{\text{Ait}}$  and  $N_{\text{Acc}}$  was  $(2.32 \pm 1.59) \times 10^3 \text{cm}^{-3}$ ,  $(3.62 \pm 1.95) \times 10^3 \text{cm}^{-3}$  and  $(1.32 \pm 0.75) \times 10^3 \text{cm}^{-3}$ , contributing 32.1%, 49.9% and 18.0% to total concentration (Fig. 1d), respectively. Nucleation mode particles are mainly derived from primary emissions and new particle formation (Kulmala, 2003; Zimmerman et al., 2020), and Aitken mode particles were mainly influenced by traffic emissions (Cai et al., 2020; Pikridas et al., 2015) and the growth of nucleation mode particles (Kulmala et al., 2004). Nucleation and Aitken mode particles constitute most of the particle number concentrations, this result indicated that the particles are mainly derived from nucleation progress and primary emissions in Xiamen wintertime, 2019.

The mean PNSD in this study was unimodal distribution, and the highest value was  $7456.17 \text{cm}^{-3}$  at 24.6 nm (Fig. 1a). The diurnal variation of PN during the measurement is shown in Fig. 1b. The increasing of  $N_{\text{nuc}}$  and  $N_{\text{Ait}}$  during the morning rush hours may be possibly caused by primary traffic emissions. According to the former researches, particles produced by traffic emissions were within the size ranges between 6 nm and 100 nm (Cai et al., 2020; Kontkanen et al., 2020). The  $N_{\text{nuc}}$  showed a clear

**Table 1**  
Statistical analysis of particle concentration distribution in December 2019.

Mode		Number concentration (cm <sup>-3</sup> )	Surface area concentration (μm <sup>2</sup> cm <sup>-3</sup> )	Volume concentration (μm <sup>3</sup> cm <sup>-3</sup> )
Total concentration	mean	7.25 × 10 <sup>3</sup>	152.34	4.03
	stdv	3.41 × 10 <sup>3</sup>	79.97	2.19
	max	3.51 × 10 <sup>4</sup>	645.46	17.00
	median	6.90 × 10 <sup>3</sup>	130.52	3.38
	min	9.85 × 10 <sup>2</sup>	29.71	0.76
Nucleation mode (<25 nm)	mean	2.32 × 10 <sup>3</sup>	2.39	0.01
	stdv	1.59 × 10 <sup>3</sup>	1.61	0.01
	max	2.19 × 10 <sup>4</sup>	22.04	0.07
	median	1.93 × 10 <sup>3</sup>	1.99	0.01
	min	1.65 × 10 <sup>2</sup>	0.19	0.00
Aitken mode (25-100 nm)	mean	3.62 × 10 <sup>3</sup>	34.95	0.39
	stdv	1.95 × 10 <sup>3</sup>	18.79	0.21
	max	1.75 × 10 <sup>4</sup>	188.92	2.25
	median	3.36 × 10 <sup>3</sup>	31.99	0.35
	min	4.49 × 10 <sup>2</sup>	4.04	0.04
Accumulation mode (100-300 nm)	mean	1.32 × 10 <sup>3</sup>	115.00	3.36
	stdv	7.60 × 10 <sup>2</sup>	64.92	2.03
	max	7.24 × 10 <sup>3</sup>	544.08	15.75
	median	1.08 × 10 <sup>3</sup>	95.02	3.01
	min	2.05 × 10 <sup>2</sup>	20.80	0.66

increasing trend after 10:00, and contribution to  $N_{total}$  increased significantly (Fig. 1c), then reached the peak after noon. This process is mainly related to the new particle formation and growth. When NPF event occurs, the  $N_{nuc}$  increases sharply, and then decreases as the particles gradually grow up due to the condensation and coagulation process. The increasing of the  $N_{Ait}$  around noon is related to the growth of nucleation mode particles. The continuous increase of  $N_{Ait}$  was caused by the accumulation due

to slowly developing of the boundary layer with low temperature in winter. Accumulation mode particles, correlated with primary emission (sea salt, etc.), secondary formation or long-range transport (Vu et al., 2015; Wang et al., 2013b), had a little contribution to the  $N_{total}$ , and the diurnal variation was relatively stable, with only a small peak in the morning and the late afternoon. The diurnal variation of total particle number concentration followed a similar trend with that of the nucleation mode, but Aitken mode particles are frequently the main component of total number concentration, suggesting that the significance contribution of new particle formation and growth and primary emissions of traffic to particle number concentration.

3.2. NPF events classification and frequency

According to the classification method mentioned above, we identified 12 NPF event days, which were about 41.4% of all observed days. These events were divided into two groups by analyzing the diurnal of nucleation mode particle number concentration. The event days with a well-distinguished increasement of GMD in nucleation mode at noon were classified into Class I, and the rest were Class II. Class I NPF event days were observed on 8 days, giving an occurrence rate of 27.6%, and the frequency of Class II were 13.8%.

There are some characteristics of Class I and Class II NPF events. In Class I NPF events, the particle number size distribution showed an obvious “banana shape”, and the nucleation-mode particles exhibited a clear growth process. Condensation sink was low in the occurrence of the event. In Class I NPF events, the concentration of nucleation-mode particles showed a significant peak during the morning peak hour, and the growth process of particles was not very clear. Condensation sink was higher than that of Class I NPF events in the occurrence of the event.

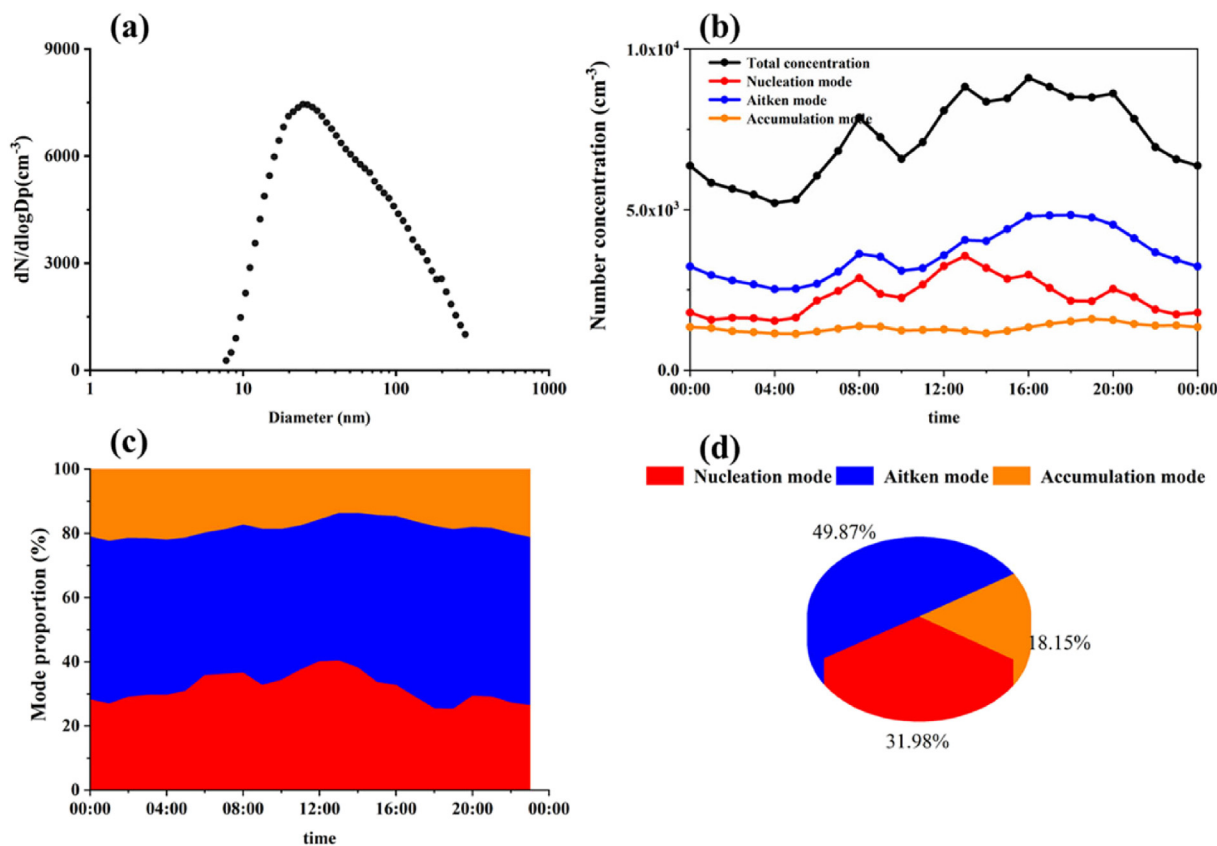


**Fig. 1.** Particle concentration distribution and diurnal variation. (a) Mean particle number size distribution, the diurnal variation of (b) number concentration and (c) the proportion of different mode, and (d) the contribution of each mode to the total particle. Different colors represent different mode particle: red (nucleation mode: 7–25 nm), blue (Aitken mode: 25–100 nm), orange (accumulation mode: 100–300 nm), and black (total: 7–300 nm). (For interpretation of the references to colour in this figure legend, the reader is referred to the web version of this article.)

The NPF frequencies in wintertime of Xiamen were much higher than in other urban sites, Shanghai (with the averaged frequency of 21% during 62-days campaign in winter (Xiao et al., 2015)) and Nanjing (with 26 days observed from 18 November 2011 to 31 March 2012 corresponds to a probability of about 20% with somewhat less during November and December (Herrmann et al., 2014)). On the other hand, NPF frequency in Xiamen was remarkably close to that measured in Beijing with a frequency of around 40% (Wu et al., 2007).

In this study, the starting time of NPF event observed was generally around 10:00 when the number concentration in nucleation mode particle increased suddenly and rapidly. We counted all NPF events and found that NPF events occurred mainly around noon. Since newly formed particles (about 1–2 nm) need some time to grow to the measurable diameter, the real start times of NPF events would be earlier than our observed times above.

The event observed on December 4 and December 14 were chosen as the representative of Class I and Class II (Fig. 2), respectively. The PNSD showed an obvious “banana shape” and the event lasted for several hours at Dec. 4th, 2019. The diurnal variation of  $N_{\text{nuc}}$  was unimodal and the peak concentration at 13:00. Followed by the increasing of  $N_{\text{nuc}}$ ,  $N_{\text{Ait}}$  slowly increased subsequently, and then a peak concentration occurred at 17:00, with a time delay of about four hours after the peak of nucleation mode particles, mainly caused by growth progress of particles from nucleation mode to a larger particle size range. Meanwhile, at Dec. 14th, 2019, the  $N_{\text{nuc}}$  appeared bimodal distribution, a small peak occurred at 8:00 and a larger one presented at 13:00. In the morning, there was an increasing of  $N_{\text{Ait}}$ , and  $\text{NO}_2$  and  $\text{CO}$  simultaneously with the increasing of  $N_{\text{nuc}}$  (Fig. S2).  $\text{NO}_2$  and  $\text{CO}$  were produced by primary emission of traffic source and industrial source respectively, thus, the first peak of particle number concentration might result from the combined effect of primary emission and no uplifted boundary layer. The  $N_{\text{nuc}}$  starts to increase once again around 11:00, and then reached the second concentration peak concentration at 13:00. During this progress, the concentration of  $\text{SO}_2$  decreased firstly and then remained stable, indicating that this is a NPF event, and sulfuric acid participated in and played a positive role in the process.

To further investigate the difference between the two types of NPF event, the meteorological parameters and pollutants were analyzed. As shown in Fig. 3, the air temperature and UV increased along with the decreased relative humidity when NPF events occurred. UV showed a usual noon peak, indicating that with sufficient sunlight and dry air could conduce to the formation of new particles. On Dec. 4th, the wind speed stayed around  $5 \text{ m s}^{-1}$ , and the prevailing wind direction was northwest. On Dec. 14th, the wind speed was varied from 1 to  $2 \text{ m s}^{-1}$  before 10:00 and the main wind direction was northwest, which were favorable for the accumulation of pollutants, after that wind speed increased to more than  $3 \text{ m s}^{-1}$ , accompanied by a decrease of  $\text{SO}_2$  and  $\text{PM}_{2.5}$  concentration. On Dec. 4th,  $\text{SO}_2$  concentration varied between 4 and  $7 \mu\text{g m}^{-3}$ , and showed minor enhancements during morning and evening hours, associated with the traffic hours. The CS was less than  $1 \times 10^{-2} \text{ s}^{-1}$ , and lower prior to the beginning of NPF event. The  $\text{O}_3$  concentration was relatively high with a mean value of  $106 \mu\text{g m}^{-3}$  and its peak occurred in the noontime with strong photochemistry reaction. The mean concentration of  $\text{PM}_{2.5}$  was  $19.2 \mu\text{g m}^{-3}$ , and secondary water-soluble inorganic ions (SNA, including  $\text{SO}_4^{2-}$ ,  $\text{NO}_3^-$  and  $\text{NH}_4^+$ ) were the main components of  $\text{PM}_{2.5}$ , therein,  $\text{SO}_4^{2-}$  is the largest contributor to atmospheric  $\text{PM}_{2.5}$ . Compared to Dec. 4th,  $\text{SO}_2$ , CS and  $\text{PM}_{2.5}$  showed sharp increase in the morning hours on Dec. 14th, which was caused by traffic emissions and accumulation of pollutants under stable meteorological with lower wind speed. Subsequently, pollutants concentration was reduced by diffusion and dilution under the high wind speed and unstable meteorological. The high pre-existing aerosol concentrations were considered unfavorable for the formation and growth of newly formed particles due to a high condensation sink (Kulmala et al., 2017). Therefore, when NPF event occurs under relative pollution conditions, the high concentrations of low volatile condensable vapors are required in atmosphere. The  $\text{O}_3$  concentration was lower on Dec. 14th, but at a higher level during the NPF event progress. Thus, the atmospheric  $\text{O}_3$  could be considered as a positive parameter that can promote the occurrence of NPF events. The  $\text{PM}_{2.5}$  concentration was at a high level with average value of  $32.8 \mu\text{g m}^{-3}$ , and the main components were  $\text{SO}_4^{2-}$ ,  $\text{NO}_3^-$ , and  $\text{NH}_4^+$ .  $\text{NO}_3^-$  was the largest contributor to the increase in  $\text{PM}_{2.5}$ , contributing about 40%.  $\text{Cl}^-$  concentration also increased during the period of high  $\text{PM}_{2.5}$  concentration.

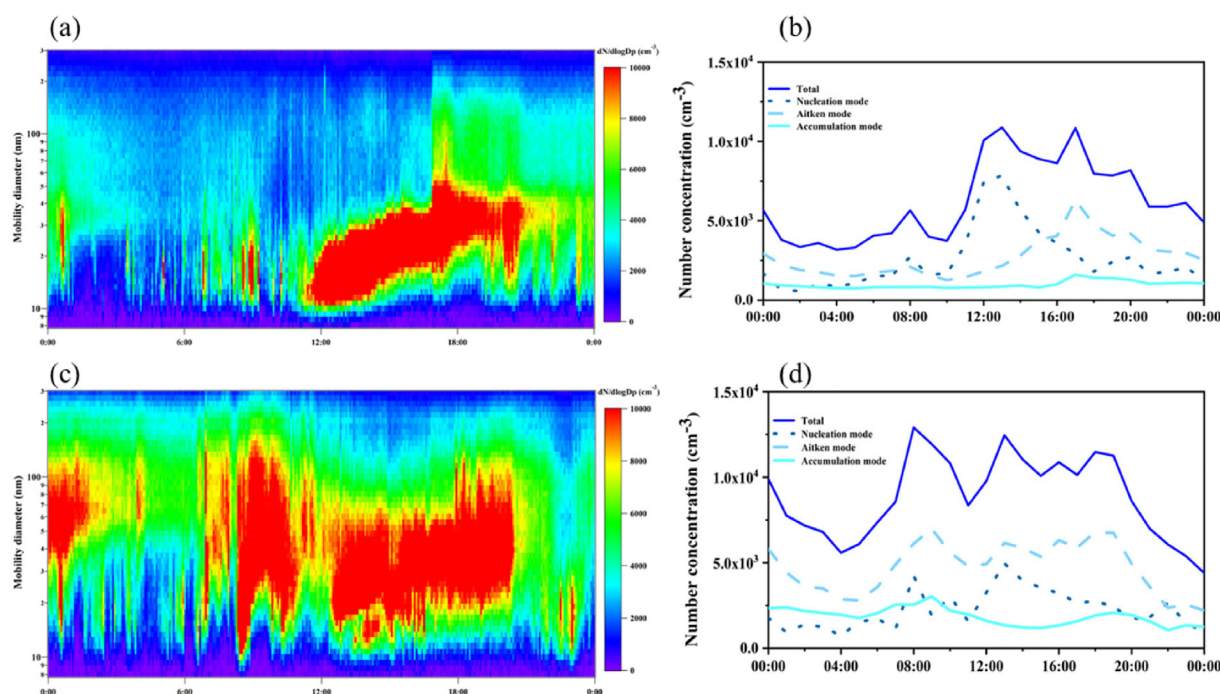


Fig. 2. Example of new particle formation (NPF) events: the particle number size distribution spectrum and number concentration of three particle size mode of Class I (a, b) and Class II (c, d).

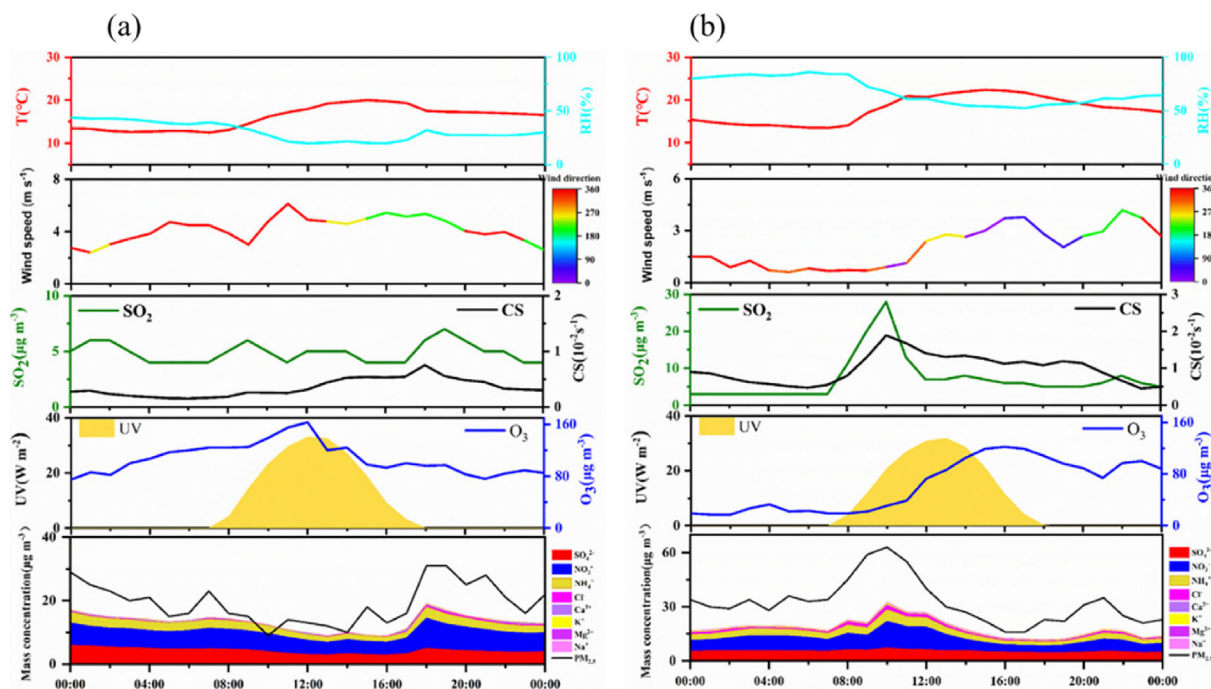


Fig. 3. Diurnal variation of meteorological parameters and pollutants in Dec. 4th, 2019 (a) and Dec. 14th, 2019 (b).

### 3.3. Formation rate and growth rate

The FR were in the range of 0.49–1.43 cm<sup>-3</sup> s<sup>-1</sup>, and the average value was 0.94 cm<sup>-3</sup> s<sup>-1</sup>. The monthly mean GR was 1.95 nm h<sup>-1</sup> with an overall variation in the range of 1.41 to 2.54 nm h<sup>-1</sup>, which were consistent with typical value found for the boundary layer (Kulmala et al., 2004). The CS varied between 0.05 × 10<sup>-2</sup> and 3.87 × 10<sup>-2</sup> s<sup>-1</sup>, and the monthly mean was 0.67 × 10<sup>-2</sup> s<sup>-1</sup>. The characteristic of FR, GR and CS during the observed NPF events are summarized in Table 2.

The FR were at the same level with those obtained at Beijing (Zhu et al., 2017), Nanjing (Herrmann et al., 2014), and Hongkong (Wang et al., 2014a) during winter, but much lower than those calculated at Nanjing and Shanghai (Xiao et al., 2015) at the particle sizes below 2 nm. The particle GRs were lower than other urban sites, for example Jordan (Hussein et al., 2020), Jiaxing (Shen et al., 2016) and Taipei (Cheung et al., 2013). The range of GR values were comparable to those obtained at Mt. Tai (1.98 ± 1.27 nm h<sup>-1</sup>), as well as to observation for other urban site, like in North Carolina State University's (NCSU) Campus with the value of 3.1 ± 2.2 nm h<sup>-1</sup> (Zimmerman et al., 2020).

As shown in Table 3, corresponding parameters observed in other studies are listed. The FR value ranged from 0.8 cm<sup>-3</sup> s<sup>-1</sup> to 271.0 cm<sup>-3</sup> s<sup>-1</sup> in urban areas, while the FR values for other areas ranged from 1.0 cm<sup>-3</sup> s<sup>-1</sup> to 33.2 cm<sup>-3</sup> s<sup>-1</sup>. FR values are higher in urban areas than in other regions, and when the particle size is small, the FR value is relatively large. As for GR, the value varied from 2.2 nm h<sup>-1</sup> to 38.7 nm h<sup>-1</sup> in urban areas, while varied from 1.8 nm h<sup>-1</sup> to 8.5 nm h<sup>-1</sup> in urban areas. The FR and GR are depending on the size of the particles and the different atmospheric environment conditions. According to the systematic reviewed by Chu et al. (2019) and Nieminen et al. (2018), the FR varied from less than 0.1 cm<sup>-3</sup> s<sup>-1</sup> to about 10<sup>3</sup> cm<sup>-3</sup> s<sup>-1</sup> with the particle size ranging from more than

10 nm to less than 2 nm, and FR tended to increase with increasing degree of anthropogenic influence at a given particle size range and were 1 to 2 orders of magnitude higher in urban areas compared to vast majority of remote and polar areas. GR varied greatly from urban to rural and from spring to winter, ranging from few to more than 20 nm h<sup>-1</sup>, with the highest value in summer and the lowest value in winter for most sites.

Whether an NPF event occurs depends on the competition between sinks and sources (Zhang et al., 2012). In this study, CS on NPF event days varied from 0.07–2.06 × 10<sup>-2</sup> s<sup>-1</sup>, corresponding to the median, 25th percentile, and 75th percentile of 0.50 × 10<sup>-2</sup>, 0.27 × 10<sup>-2</sup> and 0.80 × 10<sup>-2</sup> s<sup>-1</sup>, which was similar to values in Beijing on NPF event days (Wu et al., 2007). Although in high CS environment, NPF events still occurred frequently. This finding is consistent with the previous results reported in Chinese urban areas, such as in Beijing, Nanjing and Shanghai (Kulmala et al., 2017; Zhang et al., 2021). The higher NPF frequency could have results from an abundance of precursors, such as SO<sub>2</sub>.

### 3.4. Favorable conditions for new particle formation

To further study the favorable conditions for the occurrence of NPF event, the daily variation of meteorological conditions and pollutants concentrations during NPF days and non-NPF days were plotted in Fig. 4. Favorable meteorological conditions would promote the occurrence of NPF events, when the precursor concentrations are insufficient in the atmosphere, especially. In our study, all the NPF events occurred on sunny days.

Class I and Class II NPF event days had a similar diurnal variation trend of air temperature, and both of them were significantly higher than that of non-NPF days, indicating that the high air temperature was favorable for the occurrence of NPF events in winter. This result was in good agreement with many previous observations (Dada et al., 2017; Qi et al., 2015; Wang

Table 2

Summary of averages, medians, 25th percentiles, 75th percentiles, minima, and maxima for the NPF parameters.

	Mean	Minimum	Maximum	25th percentile	Median	75th percentile
J (cm <sup>-3</sup> s <sup>-1</sup> )	0.94	0.49	1.43	0.70	0.79	1.27
GR (nm h <sup>-1</sup> )	1.95	1.41	2.54	1.52	1.89	2.44
CS (10 <sup>-2</sup> s <sup>-1</sup> )	0.56	0.07	2.06	0.27	0.50	0.80

**Table 3**  
Comparison of NPF characteristics between this study and other studies.

Observation site	FR ( $\text{cm}^{-3} \text{s}^{-1}$ )	GR ( $\text{nm h}^{-1}$ )	Frequency	Observation time	reference
Xiamen (urban site)	0.94 ( $J_7$ )	1.95 ( $\text{GR}_{7-25}$ )	41%	December 2019	In this study
Mt. Tai (Mountain site)	$7.10 \pm 5.39$ ( $J_3$ )	$1.98 \pm 1.27$ ( $\text{GR}_{3-20}$ )	40%	Jul - Dec 2014 and Jun- Aug 2015	(Lv et al., 2018)
Beijing (urban site)	Spring: 5–12.2 ( $J_8$ ) Winter: 0.8–11 ( $J_8$ )	Spring: 2.2–9.3 ( $\text{GR}_{8-20}$ )	Spring: 43.75% Winter: 50%	10–23 December 2011; 12–27 April 2012	(Zhu et al., 2017)
Amman-Jordan (urban site)	$1.9 \pm 1.1$ 1.6–2.7 ( $J_{10}$ )	$6.8 \pm 3.1$ (4.1–8.8)	34%	August 2016–July 2017	(Hussein et al., 2020)
Shanghai (urban site)	112.4–271.0 ( $J_{1,34}$ ) 2.3–19.2 ( $J_3$ )	4.5–38.3 ( $\text{GR}_{7-20}$ )	~21%	November 2013–25 January 2014	(Xiao et al., 2015)
SORPES-NJU (suburban site)	33.2 ( $J_2$ ) 1.1 ( $J_6$ )	8.5 ( $\text{GR}_{6-30}$ ) 6.3 ( $\text{GR}_{3-7}$ ) 8.0 ( $\text{GR}_{7-30}$ )	20%	18 November 2011–31 March 2012	(Herrmann et al., 2014)
Jiaxing (urban site)	4.0–17.0 (average 9.6)	2.5–15.7 (average 6.8)	~ 48%	May 2015	(Shen et al., 2016)
Hongkong (Mountain site)	1.0–6.9 ( $J_{5,5}$ )	1.8–8.4	~ 33%	25 October - 29 November 2010	(Guo et al., 2012)
Taipei (urban site)	1.4–12.5 ( $6.9 \pm 3.0$ )	4.4–38.7 ( $11.9 \pm 10.6$ )	36%	4–29 July 2012	(Cheung et al., 2013)
Hongkong (urban site)	1.2–2.3 ( $J_{5,5}$ )	3.7–8.3 ( $\text{GR}_{5,5-10}$ )		22 December 2010–20 January 2011	(Wang et al., 2014a)

et al., 2014b). According to classical binary or ternary nucleation, water vapor can directly participate in nucleation progress (Duplissy et al., 2016), however, studies have found that high RH is not conducive to new particle generation (Cai et al., 2017; Li et al., 2019). Therefore, the actual role of RH has always been controversial. The relative humidity of Class I event days was greatly lower than that of non-NPF days. Although the relative humidity of Class II event days showed a similar diurnal variation trend as that of non-NPF days, the events occurred

during a period of decreasing RH, which indicated that NPF events favored low RH in Xiamen. As discussed in Section 3.2, NPF events initiated at the same time as rapid enhancement of UV radiation, suggesting that there was a promoting relationship between UV radiation and NPF (Bousiotis et al., 2021a; Dada et al., 2017). Indeed, the UV radiation on NPF events was higher than that on non-NPF event days, thereby, the photochemical process might be the main driving force of NPF.

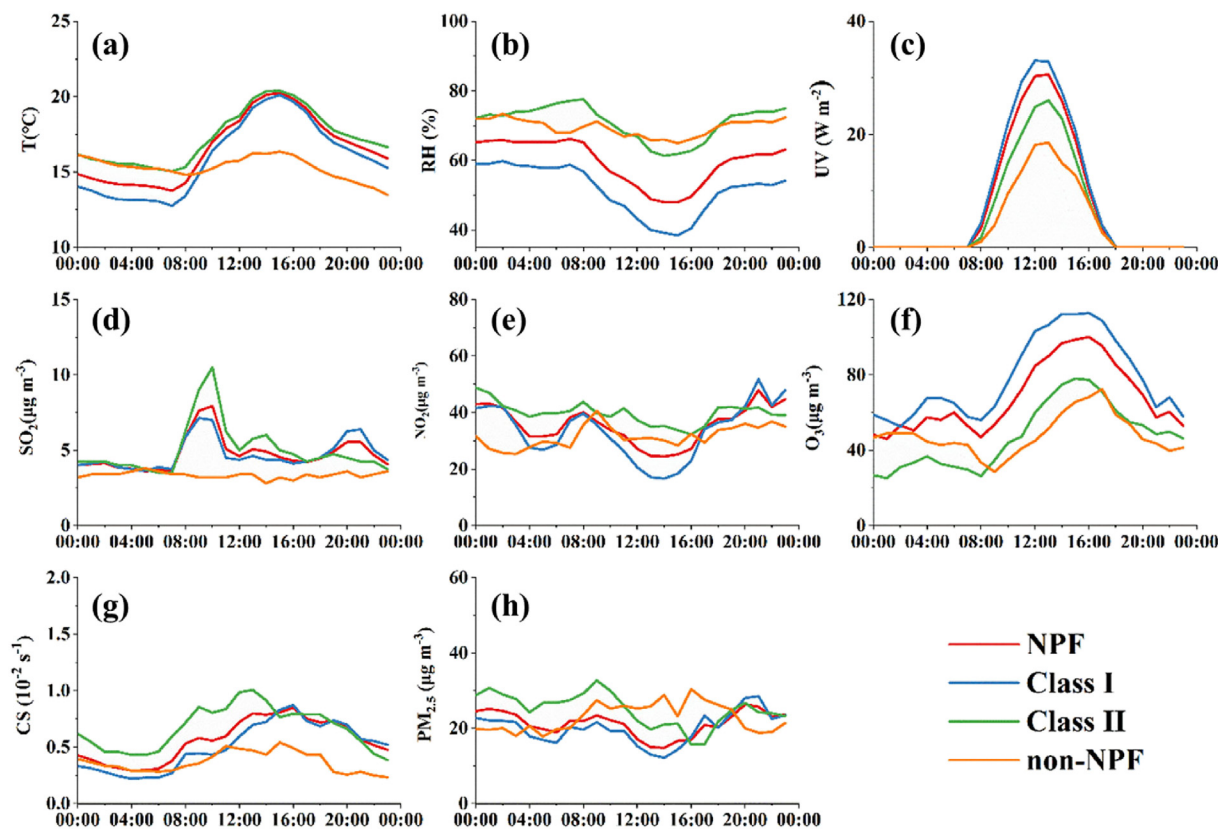


**Fig. 4.** The average diurnal variation of meteorological parameters and pollutants during NPF events (red lines), Class I NPF events (light blue lines), Class II NPF events (green lines) and non-NPF events (orange lines) in December 2019. (a) air temperature, (b) relative humidity, (c) UV radiation, (d)  $\text{SO}_2$ , (e)  $\text{NO}_2$ , (f)  $\text{O}_3$ , (g) CS, and (h)  $\text{PM}_{2.5}$ . (For interpretation of the references to colour in this figure legend, the reader is referred to the web version of this article.)

Wind direction and wind speed have some effect on the PNSD and pollutant concentration at observation sites. The dominant wind directions were north-northwest and east-northeast in non-NPF days. Compared with non-NPF event days, the prevailing wind directions on NPF days was north-northwest direction. In general, the probability of NPF events occurring in cleaner air mass is higher, while the GR of more polluting air mass is higher (Bousiotis et al., 2021b).

Gas-phase sulfuric acid has been identified as the most important precursor for nucleation (Olin et al., 2020; Yao et al., 2018), and the photochemical reaction of SO<sub>2</sub> would be the significant source for sulfuric acid in the atmosphere (Kerminen et al., 2018). SO<sub>2</sub> concentration showed a sharp increase trend on NPF days were higher than the corresponding values on non-NPF event days. This indicated that sulfuric acid participated in NPF and played an important role for NPF process. Studies at a high-altitude background site Mt. Yulong (Shang et al., 2018), a clean coastal environment of the south-wester Europe (Adame et al., 2020) and urban Shanghai (Xiao et al., 2015) have also reported anthropogenic SO<sub>2</sub> as the controlling factor of NPF.

O<sub>3</sub> in the atmosphere can enhance the formation of sulfuric acid by generating hydroxyl radicals during photolysis, thus O<sub>3</sub> may play a promoting role in NPF (Huang et al., 2016; Lv et al., 2018; Zhao et al., 2015). Atmospheric photochemical oxidant (O<sub>x</sub>) is one of the main indicators of atmospheric oxidation capacity (Herndon et al., 2008). The O<sub>3</sub> and O<sub>x</sub> concentration of Class I event days were greatly higher than that of non-NPF days, indicating that atmosphere in Class I event days had a higher oxidation capacity for the secondary transformation of pollutants (Shang et al., 2018). Although the diurnal variation trend of O<sub>3</sub> concentration on Class II event days was similar to that of non-NPF days, the average O<sub>3</sub> concentration was higher. Recently study has found that the high NO<sub>x</sub> concentration was not conducive to O<sub>3</sub> formation (Lv et al., 2018), which could be an explanation for the low O<sub>3</sub> concentration on Class II event days. The average NO<sub>2</sub> was lower on event day than that on non-NPF event day during daytime. These results showed that NO<sub>2</sub> inhibits the occurrence of NPF events by reducing O<sub>3</sub> concentration.

The average CS during Class I events were lower than that of Class II events, however, both of them were significantly higher than that of non-NPF days. Previous studies had shown that high CS would be unfavorable for the occurrence of NPF events (Cai et al., 2017), but we also found NPF events at high CS. Under the atmospheric combined pollution condition in China, NPF events often occur even with the high CS. One explanation is that heavily contaminated sites usually correspond to higher CS, so to some extent high concentrations of precursor are required to initiate nucleation (Lv et al., 2018). The mass concentration of PM<sub>2.5</sub> during Class I events were lower than that of Class II events, suggesting that Class I events were more likely to occur in clean environments. On the whole, PM concentration were lower on NPF days than that on non-NPF days, this finding is consistent with the previous results reported in the Yangtze River Delta (Shen et al., 2016).

#### 4. Conclusion

In this study, the particle size distribution, meteorological parameters, gaseous pollutant, PM<sub>2.5</sub> and the chemical composition were observed in Xiamen in wintertime (December 2019). The particle size distribution was characterized, the main contributor to particle surface area and volume concentration was particles in accumulation mode, whereas number concentration was mainly influenced by the nucleation mode and the Aitken mode particles, especially Aitken mode particles. The dynamic behavior of PNSD in the urban atmosphere in Xiamen was affected by new particle formation and subsequent growth, primary emission and local meteorological conditions.

An unexpected high NPF frequency with about 41.4% was found in our study. Two types of NPF days were observed, Class I showed an apparent growth pattern and occurred on 8 days of 12 NPF event days, while Class II without clear growth of GMD in nucleation mode occurred on 4 days of 12 NPF event days. The starting time of NPF event observed was generally around 10:00, which would be later than the real start times due to the

limitation of measured particle size range. Analysis on two different kinds of NPF events revealed that ‘banana shape’ NPF event occurred in relatively clean environment with low PM and CS. In both kinds of NPF, sufficient sunlight and dry air are conducive to the formation of new particles. The FR, GR, and CS during our measurement period were 0.94 cm<sup>-3</sup> s<sup>-1</sup>, 1.95 nm h<sup>-1</sup>, and 0.67 × 10<sup>-2</sup> s<sup>-1</sup>, respectively.

Moreover, the influence of meteorological parameters and pollutants for NPF and non-NPF days was evaluated. NPF events all occurred on no rainy days, and was favored by weather conditions with high air temperature, low relative humidity and strong UV radiation. When NPF events occurred with the high CS, a high concentration of precursors (such as SO<sub>2</sub>) was required. The concentration of SO<sub>2</sub> and O<sub>3</sub> on NPF days were higher than those on non-NPF days, but the NO<sub>2</sub> was at a low concentration level. These results indicated that SO<sub>2</sub> and O<sub>3</sub> would play a crucial part in NPF progress, NO<sub>2</sub> would suppress the occurrence of events.

Our study provided the characteristics of particle size distribution and NPF in the coastal city of Xiamen, Southeast China in wintertime. These results would improve our understanding of the characteristics particle size distribution, NPF events and their influencing factors in the coastal cities of Southeast China, and provide a basis for further study on the formation and growth mechanism of new particles formation. In future studies, nano-SMPS will be added for the study of particles with small particle size range, and more comprehensive and long-term observations focused on particles and precursors will be conducted.

#### CRedit authorship contribution statement

**Jing Wang:** Formal analysis, Investigation, Data curation, Writing – original draft. **Mengren Li:** Conceptualization, Methodology, Formal analysis, Writing – review & editing, Funding acquisition. **Lingjun Li:** Resources, Writing – review & editing. **Ronghua Zheng:** Resources, Data curation. **Xiaolong Fan:** Resources, Writing – review & editing. **Youwei Hong:** Resources, Writing – review & editing. **Lingling Xu:** Resources. **Jinsheng Chen:** Writing – review & editing, Funding acquisition. **Baoye Hu:** Resources.

#### Declaration of competing interest

The authors declare that they have no known competing financial interests or personal relationships that could have appeared to influence the work reported in this paper.

#### Acknowledgements

This study was supported by the Natural Science Foundation of Fujian Province (2020J05091), the Cultivating Project of Strategic Priority Research Program of the Chinese Academy of Sciences (XDPB1903), the FJRSM&IUE Joint Research Fund (RHZX-2019-006), the Center for Excellence in Regional Atmospheric Environment, CAS (E0L1B20201), the Xiamen Youth Innovation Fund Project (3502Z20206094), the foreign cooperation project of Fujian Province (2020I0038), and Xiamen Atmospheric Environment Observation and Research Station of Fujian Province.

#### Appendix A. Supplementary data

Supplementary data to this article can be found online at <https://doi.org/10.1016/j.scitotenv.2022.154208>.

#### References

- Adame, J.A., Lope, L., Sorribas, M., Notario, A., Yela, M., 2020. SO<sub>2</sub> measurements in a clean coastal environment of the southwestern Europe: sources, transport and influence in the formation of secondary aerosols. *Sci. Total Environ.* 716, 137075.
- Bae, M.S., Schwab, J.J., Hogrefe, O., Frank, B.P., Lala, G.G., Demerjian, K.L., 2010. Characteristics of size distributions at urban and rural locations in New York. *Atmos. Chem. Phys.* 10, 4521–4535.

- Boucher, O., Randall, D., Artaxo, P., 2013. Clouds and aerosols [M]/climate change 2013: the physical science basis. Contribution of Working Group I to the Fifth Assessment Report of the Intergovernmental Panel on Climate Change. Cambridge University Press, pp. 571–657.
- Bousiotis, D., Brean, J., Pope, F.D., Dall'Osto, M., Querol, X., Alastuey, A., et al., 2021a. The effect of meteorological conditions and atmospheric composition in the occurrence and development of new particle formation (NPF) events in Europe. *Atmos. Chem. Phys.* 21, 3345–3370.
- Bousiotis, D., Pope, F.D., Beddows, D.C.S., Dall'Osto, M., Massling, A., Nøjgaard, J.K., et al., 2021b. A phenomenology of new particle formation (NPF) at 13 European sites. *Atmos. Chem. Phys.* 21, 11905–11925.
- Cai, R., Yang, D., Fu, Y., Wang, X., Li, X., Ma, Y., et al., 2017. Aerosol surface area concentration: a governing factor in new particle formation in Beijing. *Atmos. Chem. Phys.* 17, 12327–12340.
- Cai, J., Chu, B.W., Yao, L., Yan, C., Heikkinen, L.M., Zheng, F.X., et al., 2020. Size-segregated particle number and mass concentrations from different emission sources in urban Beijing. *Atmos. Chem. Phys.* 20, 12721–12740.
- Cheung, H.C., Chou, C.C.K., Huang, W.R., Tsai, C.Y., 2013. Characterization of ultrafine particle number concentration and new particle formation in an urban environment of Taipei, Taiwan. *Atmos. Chem. Phys.* 13, 8935–8946.
- Chu, B., Kerminen, V.-M., Bianchi, F., Yan, C., Petäjä, T., Kulmala, M., 2019. Atmospheric new particle formation in China. *Atmos. Chem. Phys.* 19, 115–138.
- Dada, L., Paasonen, P., Nieminen, T., Buenrostro Mazon, S., Kontkanen, J., Peräkylä, O., et al., 2017. Long-term analysis of clear-sky new particle formation events and nonevents in Hyytiälä. *Atmos. Chem. Phys.* 17, 6227–6241.
- Dal Maso, M., Kulmala, M., Riipinen, I., Wagner, R., Hussein, T., Aalto, P.P., et al., 2005. Formation and growth of fresh atmospheric aerosols: eight years of aerosol size distribution data from SMEAR II, Hyytiälä, Finland. *Boreal Environ. Res.* 10, 323–336.
- Duplissy, J., Merikanto, J., Franchin, A., Tsagkogeorgas, G., Kangasluoma, J., Wimmer, D., et al., 2016. Effect of ions on sulfuric acid-water binary particle formation: 2. Experimental data and comparison with QC-normalized classical nucleation theory. *J. Geophys. Res.-Atmos.* 121, 1752–1775.
- Guo, H., Wang, D.W., Cheung, K., Ling, Z.H., Chan, C.K., Yao, X.H., 2012. Observation of aerosol size distribution and new particle formation at a mountain site in subtropical Hong Kong. *Atmos. Chem. Phys.* 12, 9923–9939.
- Guo, S., Hu, M., Zamora, M.L., Peng, J., Shang, D., Zheng, J., et al., 2014. Elucidating severe urban haze formation in China. *Proc. Natl. Acad. Sci. U. S. A.* 111 (49), 17373–17378.
- Hakala, S., Alghamdi, M.A., Paasonen, P., Vakkari, V., Khoder, M.I., Neitola, K., et al., 2019. New particle formation, growth and apparent shrinkage at a rural background site in western Saudi Arabia. *Atmos. Chem. Phys.* 19, 10537–10555.
- Hamed, A., Joutsensaari, J., Mikkonen, S., Sogacheva, L., Dal Maso, M., Kulmala, M., et al., 2007. Nucleation and growth of new particles in Po Valley, Italy. *Atmos. Chem. Phys.* 7, 355–376.
- Herndon, S.C., Onasch, T.B., Wood, E.C., Kroll, J.H., Canagaratna, M.R., Jayne, J.T., et al., 2008. Correlation of secondary organic aerosol with odd oxygen in Mexico City. *Geophys. Res. Lett.* 35 (15).
- Herrmann, E., Ding, A.J., Kerminen, V.M., Petäjä, T., Yang, X.Q., Sun, J.N., et al., 2014. Aerosols and nucleation in eastern China: first insights from the new SORPES-NJU station. *Atmos. Chem. Phys.* 14, 2169–2183.
- Hoffmann, T., O'Dowd, C.D., Seinfeld, J.H., 2001. Iodine oxide homogeneous nucleation: an explanation for coastal new particle production. *Geophys. Res. Lett.* 28, 1949–1952.
- Holmes, N.S., 2007. A review of particle formation events and growth in the atmosphere in the various environments and discussion of mechanistic implications. *Atmos. Environ.* 41, 2183–2201.
- Huang, X., Zhou, L., Ding, A., Qi, X., Nie, W., Wang, M., et al., 2016. Comprehensive modelling study on observed new particle formation at the SORPES station in Nanjing, China. *Atmos. Chem. Phys.* 16, 2477–2492.
- Hussein, T., Puustinen, A., Aalto, P.P., Makela, J.M., Hameri, K., Kulmala, M., 2004. Urban aerosol number size distributions. *Atmos. Chem. Phys.* 4, 391–411.
- Hussein, T., Dal Maso, M., Petaja, T., Koponen, I.K., Paatero, P., Aalto, P.P., et al., 2005a. Evaluation of an automatic algorithm for fitting the particle number size distributions. *Boreal Environ. Res.* 10, 337–355.
- Hussein, T., Hameri, K.A., Aalto, P.P., Paatero, P., Kulmala, M., 2005b. Modal structure and spatial-temporal variations of urban and suburban aerosols in Helsinki - Finland. *Atmos. Environ.* 39, 1655–1668.
- Hussein, T., Martikainen, J., Junninen, H., Sogacheva, L., Wagner, R., Dal Maso, M., et al., 2008. Observation of regional new particle formation in the urban atmosphere. *Tellus Ser.BChem.Phys.Meteorol.* 60, 509–521.
- Hussein, T., Dada, L., Hakala, S., Petaja, T., Kulmala, M., 2019. Urban aerosol particle size characterization in eastern Mediterranean conditions. *Atmosphere* 10.
- Hussein, T., Atashi, N., Sogacheva, L., Hakala, S., Dada, L., Petäjä, T., et al., 2020. Characterization of urban new particle formation in Amman—Jordan. *Atmosphere* 11.
- Kalkavouras, P., Bougiatioti, A., Hussein, T., Kalivitis, N., Stavroulas, I., Michalopoulos, P., et al., 2020. Regional new particle formation over the Eastern Mediterranean and Middle East. *Atmosphere* 12.
- Kammer, J., Perraudin, E., Flaud, P.M., Lamaud, E., Bonnefond, J.M., Villenave, E., 2018. Observation of nighttime new particle formation over the French Landes forest. *Sci. Total Environ.* 621, 1084–1092.
- Kerminen, V.-M., Chen, X., Vakkari, V., Petäjä, T., Kulmala, M., Bianchi, F., 2018. Atmospheric new particle formation and growth: review of field observations. *Environ. Res. Lett.* 13.
- Kirkby, J., Duplissy, J., Sengupta, K., Frege, C., Gordon, H., Williamson, C., et al., 2016. Ion-induced nucleation of pure biogenic particles. *Nature* 533, 521.
- Kontkanen, J., Deng, C.J., Fu, Y.Y., Dada, L., Zhou, Y., Cai, J., et al., 2020. Size-resolved particle number emissions in Beijing determined from measured particle size distributions. *Atmos. Chem. Phys.* 20, 11329–11348.
- Kulmala, M., 2003. Atmospheric science. How particles nucleate and grow. *Science* 302 (5647), 1000–1001.
- Kulmala, M., Toivonen, A., Makela, J.M., Laaksonen, A., 1998. Analysis of the growth of nucleation mode particles observed in boreal forest. *Tellus Ser.BChem.Phys.Meteorol.* 50, 449–462.
- Kulmala, M., Hameri, K., Aalto, P.P., Makela, J.M., Pirjola, L., Nilsson, E.D., et al., 2001. Overview of the international project on biogenic aerosol formation in the boreal forest (BIOFOR). *Tellus Ser.BChem.Phys.Meteorol.* 53, 324–343.
- Kulmala, M., Vehkamäki, H., Petäjä, T., Dal Maso, M., Lauri, A., Kerminen, V.M., et al., 2004. Formation and growth rates of ultrafine atmospheric particles: a review of observations. *J. Aerosol Sci.* 35, 143–176.
- Kulmala, M., Petaja, T., Nieminen, T., Sipilä, M., Manninen, H.E., Lehtipalo, K., et al., 2012. Measurement of the nucleation of atmospheric aerosol particles. *Nat. Protoc.* 7, 1651–1667.
- Kulmala, M., Petäjä, T., Kerminen, V.-M., Kujansuu, J., Ruuskanen, T., Ding, A., 2016. On secondary new particle formation in China. *Front. Environ. Sci. Eng.* 10.
- Kulmala, M., Kerminen, V.M., Petaja, T., Ding, A.J., Wang, L., 2017. Atmospheric gas-to-particle conversion: why NPF events are observed in megacities? *Faraday Discuss.* 200, 271–288.
- Li, X., Chee, S., Hao, J., Abbatt, J.P.D., Jiang, J., Smith, J.N., 2019. Relative humidity effect on the formation of highly oxidized molecules and new particles during monoterpene oxidation. *Atmos. Chem. Phys.* 19, 1555–1570.
- Liu, B.Y.H., Pui, D.Y.H., 1974. Submicron aerosol standard and primary, absolute calibration of condensation nuclei counter. *J. Colloid Interface Sci.* 47, 155–171.
- Lv, G., Sui, X., Chen, J., Jayaratne, R., Mellouki, A., 2018. Investigation of new particle formation at the summit of Mt. Tai, China. *Atmos. Chem. Phys.* 18, 2243–2258.
- McMurry, P.H., Friedlander, S.K., 1979. New particle formation in the presence of an aerosol. *Atmos. Environ.* 13, 1635–1651.
- Nel, A., Xia, T., Madler, L., Li, N., 2006. Toxic potential of materials at the nanolevel. *Science* 311, 622–627.
- Nieminen, T., Kerminen, V.M., Petaja, T., Aalto, P.P., Arshinov, M., Asmi, E., et al., 2018. Global analysis of continental boundary layer new particle formation based on long-term measurements. *Atmos. Chem. Phys.* 18, 14737–14756.
- Oberdorster, G., Oberdorster, E., Oberdorster, J., 2005. Nanotoxicology: an emerging discipline evolving from studies of ultrafine particles. *Environ. Health Perspect.* 113, 823–839.
- O'Dowd, C.D., Geever, M., Hill, M.K., 1998. New particle formation: nucleation rates and spatial scales in the clean marine coastal environment. *Geophys. Res. Lett.* 25, 1661–1664.
- O'Dowd, C.D., Jimenez, J.L., Bahreini, R., Flagan, R.C., Seinfeld, J.H., Hameri, K., et al., 2002. Marine aerosol formation from biogenic iodine emissions. *Nature* 417, 632–636.
- Olin, M., Kuuluvainen, H., Aurela, M., Kalliokoski, J., Kuittinen, N., Isotalo, M., et al., 2020. Traffic-originated nanocluster emission exceeds H<sub>2</sub>SO<sub>4</sub>-driven photochemical new particle formation in an urban area. *Atmos. Chem. Phys.* 20, 1–13.
- Penttinen, P., Timonen, K.L., Tiittanen, P., Mirme, A., Ruuskanen, J., Pekkanen, J., 2001. Number concentration and size of particles in urban air: effects on spirometric lung function in adult asthmatic subjects. *Environ. Health Perspect.* 109, 319–323.
- Pikridas, M., Sciare, J., Freutel, F., Crumeyrolle, S., von der Weiden-Reinmüller, S.L., Borbon, A., et al., 2015. In situ formation and spatial variability of particle number concentration in a European megacity. *Atmos. Chem. Phys.* 15 (17), 10219–10237.
- Qi, X.M., Ding, A.J., Nie, W., Petäjä, T., Kerminen, V.M., Herrmann, E., et al., 2015. Aerosol size distribution and new particle formation in the western Yangtze River Delta of China: 2 years of measurements at the SORPES station. *Atmos. Chem. Phys.* 15, 12445–12464.
- Qiao, X., Yan, C., Li, X., Guo, Y., Yin, R., Deng, C., et al., 2021. Contribution of atmospheric oxygenated organic compounds to particle growth in an urban environment. *Environ. Sci. Technol.* 55 (20), 13646–13656.
- Sellegri, K., Rose, C., Marinoni, A., Lupi, A., Wiedensohler, A., Andrade, M., et al., 2019. New particle formation: a review of ground-based observations at mountain research stations. *Atmosphere* 10.
- Shang, D., Hu, M., Zheng, J., Qin, Y., Du, Z., Li, M., et al., 2018. Particle number size distribution and new particle formation under the influence of biomass burning at a high altitude background site at Mt. Yulong (3410 m), China. *Atmos. Chem. Phys.* 18, 15687–15703.
- Shen, L., Wang, H., Lu, S., Li, L., Yuan, J., Zhang, X., et al., 2016. Observation of aerosol size distribution and new particle formation at a coastal city in the Yangtze River Delta, China. *Sci. Total Environ.* 565, 1175–1184.
- Shen, X., Sun, J., Ma, Q., Zhang, Y., Zhong, J., Yue, Y., et al., 2021. Long-term trend of new particle formation events in the Yangtze River Delta, China and its influencing factors: 7-year dataset analysis. *Sci. Total Environ.* 807, 150783.
- Sipilä, M., Berndt, T., Petaja, T., Brus, D., Vanhanen, J., Stratmann, F., et al., 2010. The role of sulfuric acid in atmospheric nucleation. *Science* 327, 1243–1246.
- Takegawa, N., Seto, T., Moteki, N., Koike, M., Oshima, N., Adachi, K., et al., 2020. Enhanced new particle formation above the marine boundary layer over the Yellow Sea: potential impacts on cloud condensation nuclei. *J. Geophys. Res. Atmos.* 125.
- Tang, L., Shang, D., Fang, X., Wu, Z., Qiu, Y., Chen, S., et al., 2021. More significant impacts from new particle formation on haze formation during COVID-19 lockdown. *Geophys. Res. Lett.* 48 (8) (e2020GL091591).
- Vu, T.V., Delgado-Saborit, J.M., Harrison, R.M., 2015. Review: particle number size distributions from seven major sources and implications for source apportionment studies. *Atmos. Environ.* 122, 114–132.
- Wang, Z., Hu, M., Wu, Z., Yue, D., 2013a. Research on the formation mechanisms of new particles in the atmosphere. *Acta Chim. Sin.* 71.
- Wang, Z.B., Hu, M., Wu, Z.J., Yue, D.L., He, L.Y., Huang, X.F., et al., 2013b. Long-term measurements of particle number size distributions and the relationships with air mass history and source apportionment in the summer of Beijing. *Atmos. Chem. Phys.* 13, 10159–10170.
- Wang, D., Guo, H., Cheung, K., Gan, F., 2014a. Observation of nucleation mode particle burst and new particle formation events at an urban site in Hong Kong. *Atmos. Environ.* 99, 196–205.

- Wang, H., Zhu, B., Shen, L., An, J., Yin, Y., Kang, H., 2014b. Number size distribution of aerosols at Mt. Huang and Nanjing in the Yangtze River Delta, China: effects of air masses and characteristics of new particle formation. *Atmos. Res.* 150, 42–56.
- Wang, N., Sun, X., Chen, J., Li, X., 2017. Heterogeneous nucleation of trichloroethylene ozonation products in the formation of new fine particles. *Sci. Rep.* 7, 42600.
- Wang, F., Zhang, Q.X., Xu, X.Z., Zhao, W.X., Zhang, Y.M., Zhang, W.J., 2019. Thermo-optical and particle number size distribution characteristics of smoldering smoke from biomass burning. *Appl.Sci.Basel* 9.
- Wehner, B., Wiedensohler, A., Tuch, T.M., Wu, Z.J., Hu, M., Slanina, J., et al., 2004. Variability of the aerosol number size distribution in Beijing, China: new particle formation, dust storms, and high continental background. *Geophys. Res. Lett.* 31.
- Whitby, K.T., 1978. The physical characteristics of sulfur aerosols. *Atmos. Environ.* 12 (1–3), 135–159 (1967).
- Wiedensohler, A., Ma, N., Birmili, W., Heintzenberg, J., Ditas, F., Andreae, M.O., et al., 2019. Infrequent new particle formation over the remote boreal forest of Siberia. *Atmos. Environ.* 200, 167–169.
- Wu, Z., Hu, M., Liu, S., Wehner, B., Bauer, S., Maßling, A., 2007. New particle formation in Beijing, China: statistical analysis of a 1-year data set. *J. Geophys. Res.* 112.
- Wu, Z., Hu, M., Lin, P., Liu, S., Wehner, B., Wiedensohler, A., 2008. Particle number size distribution in the urban atmosphere of Beijing, China. *Atmos. Environ.* 42, 7967–7980.
- Wu, H., Li, Z., Jiang, M., Liang, C., Zhang, D., Wu, T., et al., 2021. Contributions of traffic emissions and new particle formation to the ultrafine particle size distribution in the megacity of Beijing. *Atmos. Environ.* 262.
- Xiao, S., Wang, M.Y., Yao, L., Kulmala, M., Zhou, B., Yang, X., et al., 2015. Strong atmospheric new particle formation in winter in urban Shanghai, China. *Atmos. Chem. Phys.* 15, 1769–1781.
- Yao, L., Garmash, O., Bianchi, F., Zheng, J., Yan, C., Kontkanen, J., et al., 2018. Atmospheric new particle formation from sulfuric acid and amines in a Chinese megacity. *Science* 361, 278.
- Yue, D.L., Hu, M., Wu, Z.J., Guo, S., Wen, M.T., Nowak, A., et al., 2010. Variation of particle number size distributions and chemical compositions at the urban and downwind regional sites in the Pearl River Delta during summertime pollution episodes. *Atmos. Chem. Phys.* 10, 9431–9439.
- Zhang, R., Khalizov, A., Wang, L., Hu, M., Xu, W., 2012. Nucleation and growth of nanoparticles in the atmosphere. *Chem. Rev.* 112, 1957–2011.
- Zhang, Q., Jia, S., Yang, L., Krishnan, P., Zhou, S., Shao, M., et al., 2021. New particle formation (NPF) events in China urban clusters given by severe composite pollution background. *Chemosphere* 262.
- Zhao, S., Yu, Y., Yin, D., He, J., 2015. Meteorological dependence of particle number concentrations in an urban area of complex terrain, Northwestern China. *Atmos. Res.* 164, 304–317.
- Zhu, Y., Yan, C., Zhang, R., Wang, Z., Zheng, M., Gao, H., et al., 2017. Simultaneous measurements of new particle formation at 1 s time resolution at a street site and a rooftop site. *Atmos. Chem. Phys.* 17, 9469–9484.
- Zhu, Y., Shen, Y., Li, K., Meng, H., Sun, Y., Yao, X., et al., 2021. Investigation of particle number concentrations and new particle formation with largely reduced air pollutant emissions at a coastal semi-urban site in northern China. *J. Geophys. Res.* Atmos. 126.
- Zimmerman, A., Petters, M.D., Meskhidze, N., 2020. Observations of new particle formation, modal growth rates, and direct emissions of sub-10 nm particles in an urban environment. *Atmos. Environ.* 242, 117835.